International Journal of Science and Healthcare Research
Vol. 9; Issue: 4; October-December 2024
Website: ijshr.com
Case Report *ISSN: 2455-7587*

Yamaguchi Syndrome (Ace of Spades) in an Elderly Male. Case Report and Literature Review

Akhil Mehrotra[1], Faiz Illahi Siddiqui[2]

[1]Chief, Pediatric and Adult Cardiology, Prakash Heart Station, Nirala Nagar, Lucknow, UP, India.
[2] Cardiac Technician, Prakash Heart Station, Nirala Nagar, Lucknow, UP, India.

Corresponding Author: Dr. Akhil Mehrotra

DOI: https://doi.org/10.52403/ijshr.20240449

ABSTRACT

Apical hypertrophic cardiomyopathy (AHCM) is a rare phenotypic variant of hypertrophic cardiomyopathy (HCM), most commonly seen in Asian men (Yamaguchi syndrome). It is characterized by hypertrophy, predominantly affecting the cardiac apex, with an "ace of spades"-shaped left ventricular (LV) cavity best seen on the 4-chamber view of a transthoracic echocardiogram (TTE). However, TTE can be falsely negative in 30% of AHCM cases, largely due to difficulties in delineating endocardial border. The diagnostic criteria for apical cardiac hypertrophy are: 1) asymmetric LV hypertrophy - predominantly at the apex of the ventricle; 2) LV wall thickness of 15 mm or more during diastole; and 3) apical to posterior wall thickness ratio of 1.5 or more determined by 2-dimensional echocardiography or cardiac magnetic resonance imaging. Here, we are presenting a case of elderly male who visited our cardiac OPD for a check-up due to atypical chest pain, cough and mild fever for 5 days. His resting ECG showed left ventricular hypertrophy with deep T wave inversion in precordial leads V_2-V_6, consistent with AHCM. An exhaustive transthoracic echocardiography (TTE) with contrast study (CS) and speckle tracking imaging by 4Dimensional XStrain speckle tracking echocardiography (STE) was performed to provide a clinching diagnosis.

Keywords: Hypertrophic cardiomyopathy, Apical hypertrophic cardiomyopathy, Ace of spades, Strain echocardiography, Contrast imaging in apical hypertrophic cardiomyopathy, Yamaguchi syndrome, 4Dimensional XStrain echocardiography.

INTRODUCTION

Apical hypertrophic cardiomyopathy (AHCM) is a rare phenotypic variant of hypertrophic cardiomyopathy (HCM), most commonly seen in Asian men (Yamaguchi syndrome). Apical HCM is characterized by hypertrophy predominantly affecting the cardiac apex, with an “ace of spades”–shaped left ventricular (LV) cavity best seen on the 4-chamber view of a transthoracic echocardiogram (TTE).

However, TTE can be falsely negative in 30% of AHCM cases, largely due to difficulties in delineating endocardial border [1, 2].

Hypertrophic cardiomyopathy, an inherited heterogeneous cardiac condition with diverse phenotypic expression, is a common cause of sudden cardiac death in young adults. Apical hypertrophic cardiomyopathy (AHCM), was first described in Japan in 1976 by Sakamoto et al [3] (Figures 1- 6).

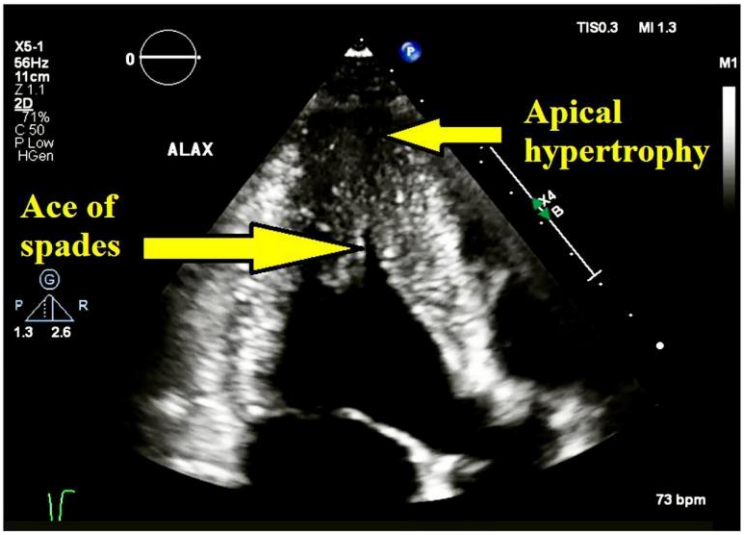

Figure 1: Transthoracic echocardiography. Apical 3CH view delineates the typical features of AHCM with "ace of spades" like LV cavity.

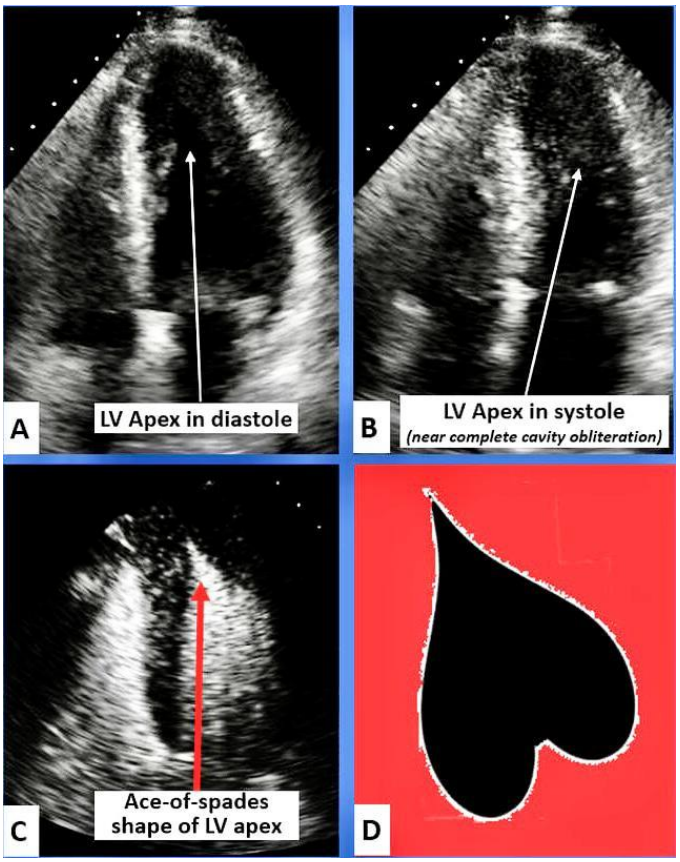

Figure 2: AHCM - Contrast echocardiography. The figure above shows 2-D echocardiographic images in apical hypertrophic cardiomyopathy. Figure A shows the thickening of the mid to apical wall segments of the left ventricle (LV) in diastole, while figure B shows the near complete obliteration of the LV apical cavity in systole due to the hypertrophy. Figure C demonstrates characteristic Ace-of-spades appearance of the LV using contrast, as depicted in the cartoon in figure D.

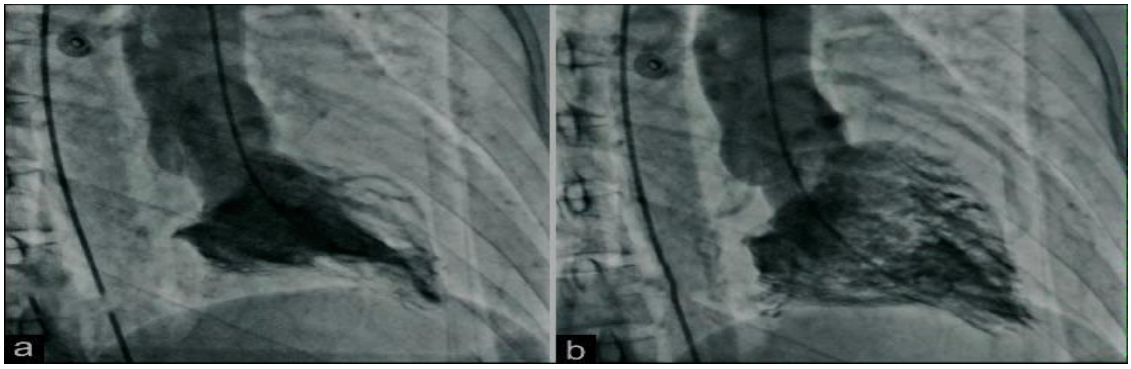

Figure 3: Ventriculogram showing left ventricle apical hypertrophy with spade-like configuration of the ventricular cavity during systole (a) and diastole (b).

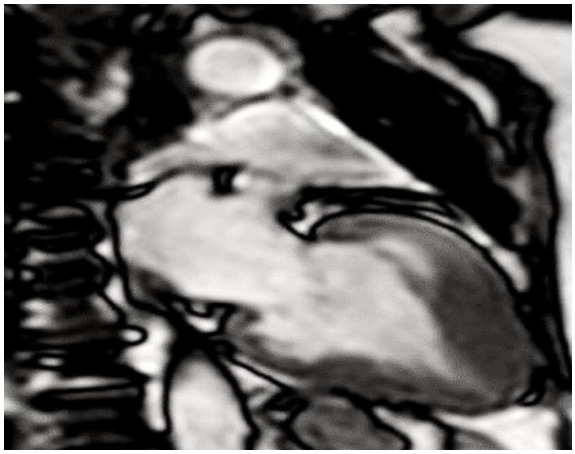

Figure 4: Cardiac MRI ace of spades sign in Yamaguchi syndrome.

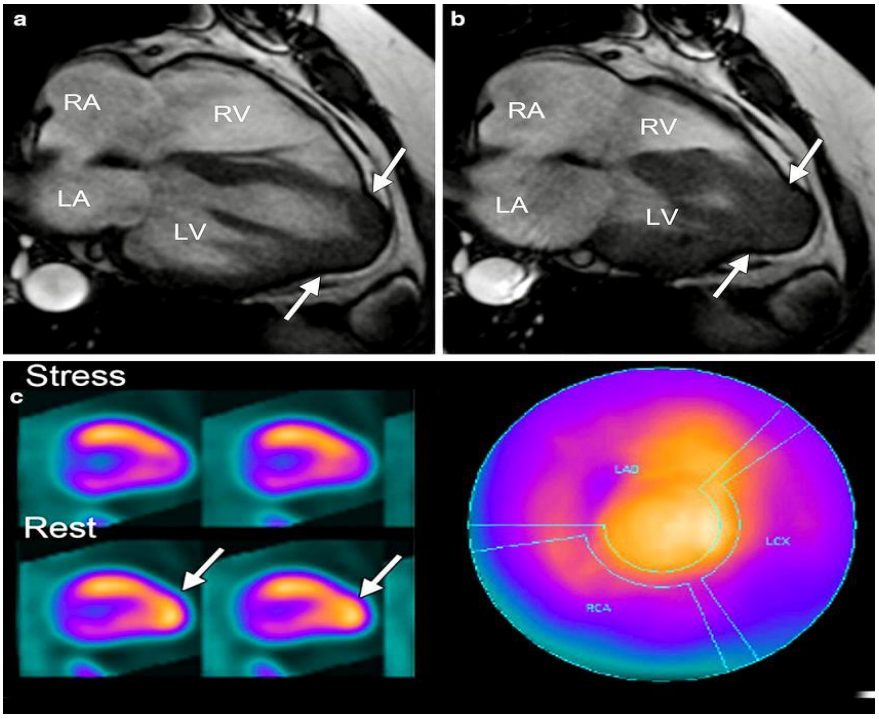

Figure 5: Apical hypertrophic cardiomyopathy- myocardial perfusion scintigraphy. (a) Four-chamber view SSFP CMR at end-diastole and (b) during systole show left ventricular myocardial thickening (white arrows) more pronounced at the apex with almost obliteration of the cavity during systole. (c) Myocardial perfusion scan with evidence of mild ischemia during stress at the inferior wall and at the apex. Notice more counts at the apex during rest (white arrows) with "solar polar map pattern" on the Bull's eye image.

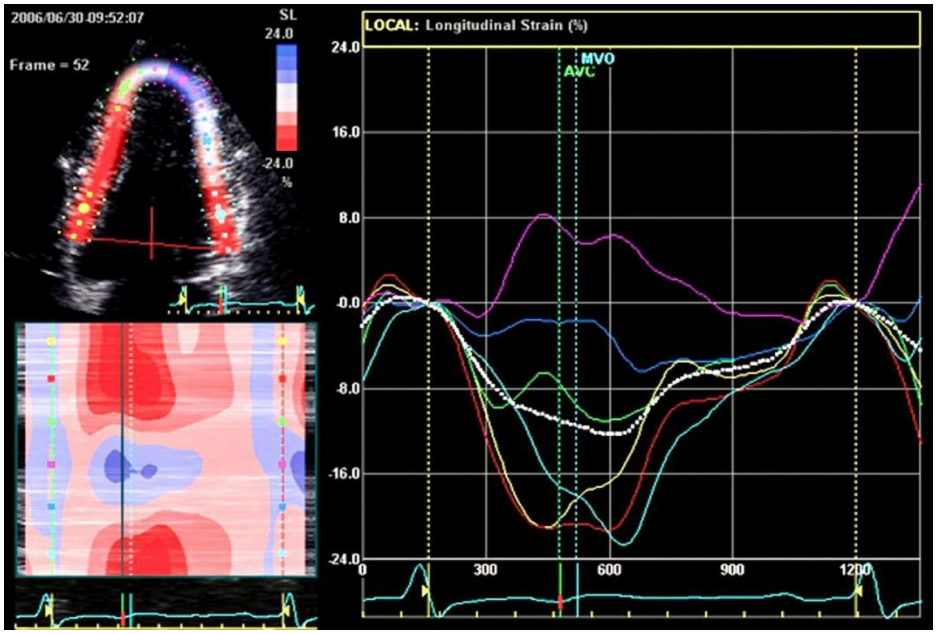

Figure 6: Apical four-chamber view showing longitudinal strain curves alongside curved anatomical M-mode of the parametric image depicting paradoxical apical strain.

AHCM typically demonstrates giant negative precordial T waves in the resting ECG. In AHCM, hypertrophy is localized to the left ventricular apex with or without midsegment or basal involvement and with or without apical aneurysm [4].

Typically, there is no LV outflow tract obstruction from systolic anterior motion of the anterior mitral valve leaflet in AHCM and it can exist with or without midventricular obstruction and cavity obliteration (MVOCO) [1].

AHCM is distributed worldwide, affecting more men than women. It is typically diagnosed in midlife [5, 6]. However, it can be diagnosed late in life and can carry a normal life expectancy. We report a case of asymptomatic AHCM presenting to us at the age of 76 years.

CASE REPORT

A 76-year elderly male presented to our cardiology OPD for a check-up due to atypical chest pain, cough and mild fever since last 5 days. The patient denied any history of cardiovascular risk factors (smoking, tobacco chewing, hypertension, diabetes, dyslipidemia).

On clinical examination, the patient was healthy looking and normally built (Figure 7). The patient's weight was 73 kg, height was 156 cm, pulse rate was 69/min, blood pressure was 130/80 mmHg, respiratory rate was 16/min and SPO2 was 98% at room air. All the peripheral pulses were normally palpable without any radio-femoral delay. Cardiovascular and systemic examination were normal.

Figure 7: Facial appearance of the elderly gentleman

Xray chest (PA) view (Figure 8) showed a normal cardiac size with a non-homogeneous opacity in the lower zone of right lung, suggestive of pneumonitis patch.

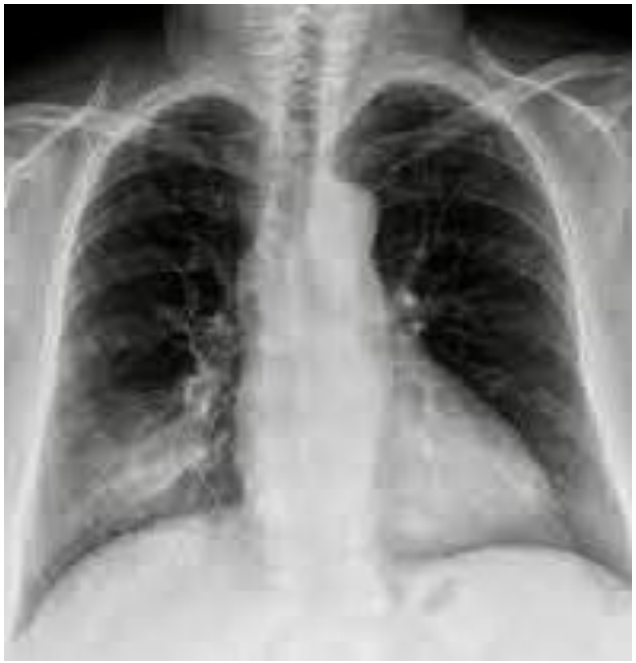

Figure 8: X-ray chest (PA view). The cardiac size is normal with normal pulmonary blood flow. A non-homogeneous opacity is visualized in the lower zone of right lung suggestive of pneumonitis patch.

The resting ECG (Figure 9) revealed classical features of LVH with deep T wave inversion in precordial leads V_2-V_6, consistent with apical hypertrophic cardiomyopathy.

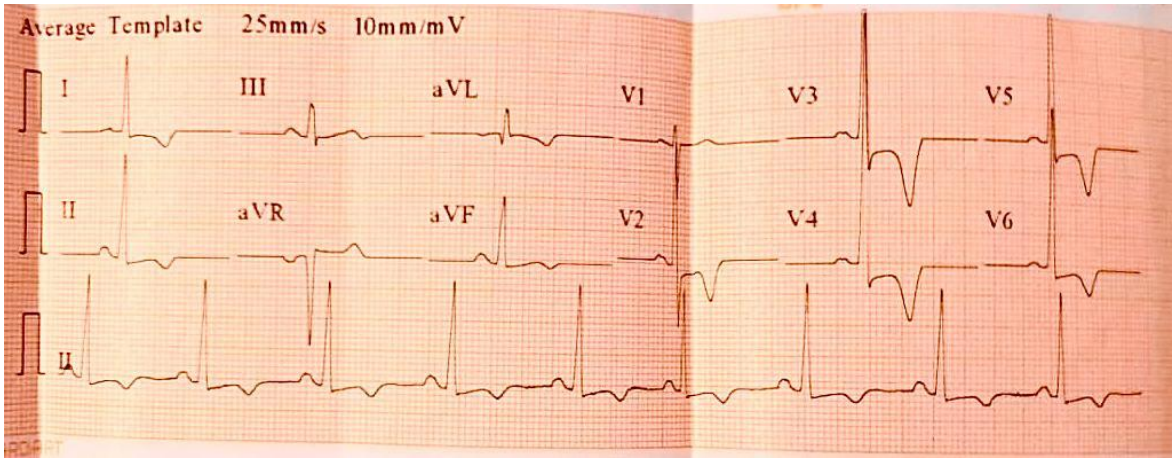

Figure 9: Resting ECG. Classical ECG features of apical hypertrophic cardiomyopathy is elucidated accompanied by left ventricular hypertrophy. The conspicuous deep T wave inversion in the precordial leads V2- V6 is striking. There is normal sinus rhythm with a ventricular rate of 70/min and normal QRS axis.

Transthoracic Echocardiography

All echocardiography evaluations were performed by the author, using My Lab X7 4D XStrain echocardiography machine, Esaote, Italy. The images were acquired using an adult probe equipped with harmonic variable frequency electronic single crystal array transducer while the subject was lying in supine and left lateral decubitus positions.

Conventional M-mode, two-dimensional, pulse wave doppler (PWD) and continuous wave doppler (CWD) echocardiography was performed in the classical subcostal,

parasternal long axis (LX), parasternal short axis (SX), 4-Chamber (4CH), 5-Chamber (5CH) and suprasternal views (Figures 10-18).

M-mode Echocardiography

M-mode echocardiography of left ventricle was performed and the estimated measurements are outlined (Table 1, Figure 10).

Table 1: Calculations of M-mode echocardiography

Measurements	LV
IVS d	12.7 mm
LVID d	45.8 mm
LVPW d	10.3 mm
IVS s	15.8 mm
LVID s	23.4 mm
LVPW s	18.6 mm
EF	80 %
% LVFS	49 %
LVEDV	96.3 ml
LVESV	18.9 ml
SV	77.4 ml
LV Mass	192 g

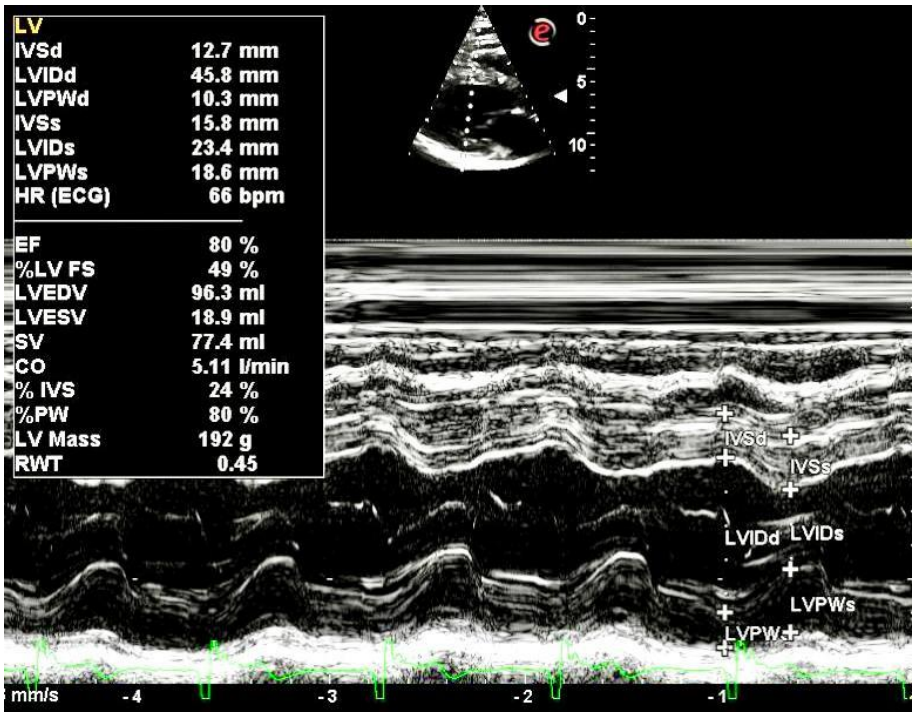

Figure 10: M-mode measurements of left ventricle

Summary of M-mode echocardiography

The LV was of normal size and the LVEF was 80 %. There was asymmetrical septal hypertrophy: interventricular septal thickness and posterior wall thickness was 12.7 mm and 10.3 mm respectively. There was no apparent regional wall motion abnormality.

2Dimensional transthoracic echocardiography

In the LX view, there was conspicuous presence of asymmetrical septal hypertrophy (Figure 11).

IVS thickness basal	(D) 14.7 mm
Mid	(D) 18.0 mm
Apical	(D) 15.4 mm
LVPW thickness	(D) 10.0 mm
IVS/LVPW ratio = 1.8:1	

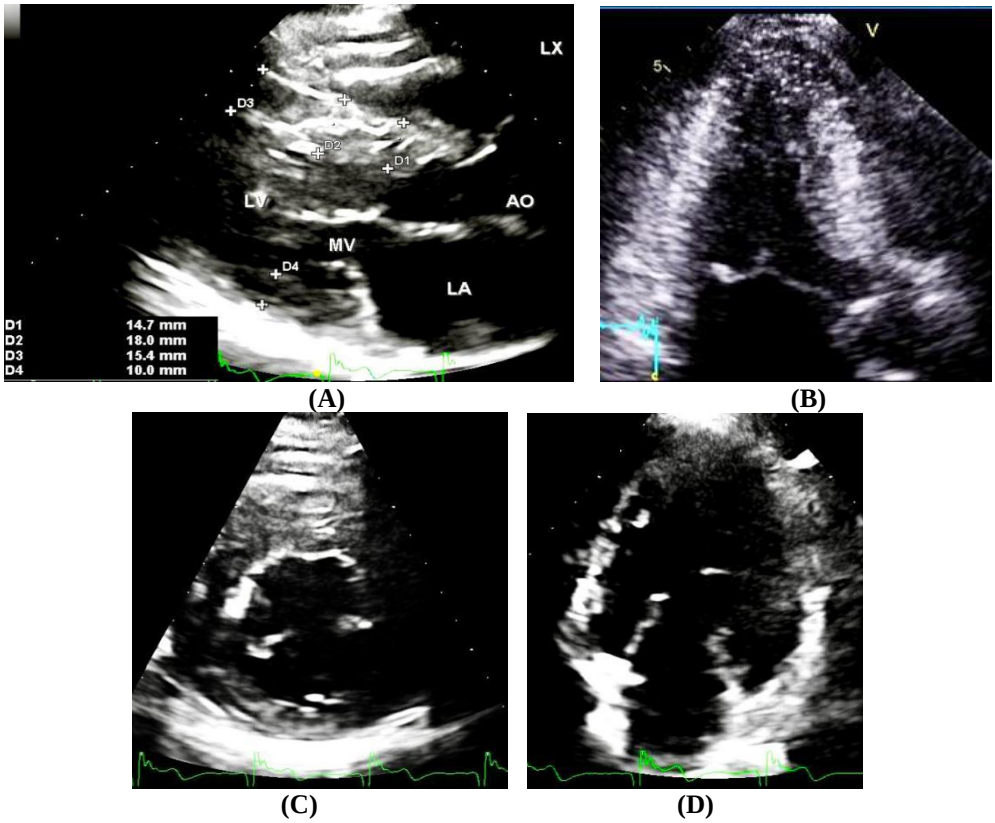

Figure 11: 2Dimensional Transthoracic Echocardiography. (A) LX view; (B) Apical 3CH view (LAX view); (C) SX view at the level of papillary muscle; (D) Apical 4CH view - large elongated AML and PML are visualized.

Additionally, other important echocardiographic findings are mentioned below:

- Markedly thickened LV apex and apical lateral wall was appreciated.
- There was no SAM/LVOT obstruction/MVP.
- LVEF was normal
  M-mode - 80 %
  Simpson's biplane method - 51 % (Figure 12).
- Mitral regurgitation (mild) was present (Figure 13);
  MV was thickened, MR velocity was 4.42 m/sec
  On color flow mapping MR JET area was 1.10 sq cm; 10 % of LA area, eccentric posterior jet.
- The dimensions of LV were normal and there was no regional wall motion abnormality.
- Mild PAH was present and estimated RVSP/PAP was 37 mmHg.
- Pulse wave doppler analysis across the mitral valve and tissue doppler imaging of the base of lateral wall of LV were un-remarkable (Figure 14).

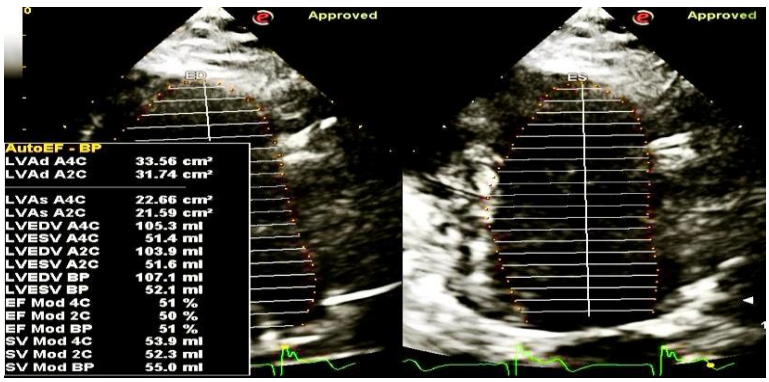

Figure 12: Simpson's biplane method- LVEF 51 %.

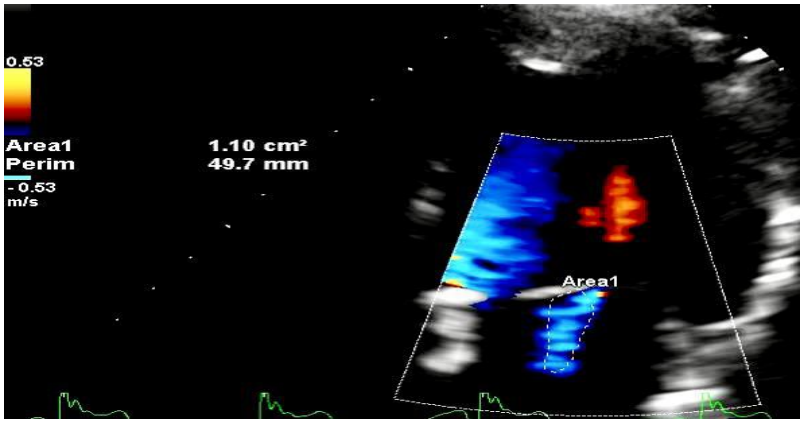

Figure 13: Mild mitral regurgitation is identified with a jet area of 1.10 sqcm and a central jet.

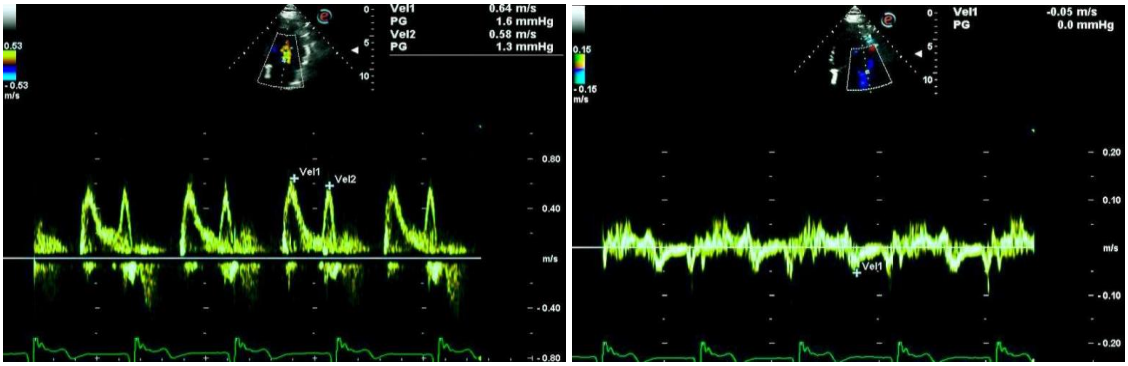

(A) **(B)**

Figure 14: (A) Pulse wave Doppler across mitral valve; (B) Tissue Doppler imaging of the base of lateral LV.

4Dimensional volumetric data

Table 2 depicts the 4Dimensional volumetric data (Figure 15)

Table 2: 4Dimensional volumetric data

Parameters	Values
LVEDV	109.40 ml
LVESV	67.24 ml
EF	38.54 %
CO	2593.62 ml/min
Sph i d	0.56
Sph i s	0.42
EDV, end diastolic volume; ESV, end systolic volume; EF, ejection fraction; CO, cardiac output; Sph i d, sphericity index diastole; Sph i s, sphericity index systole	

Interestingly, the 4Dimensional LVEF acquired from 4Dimensional STE was 38.54%.

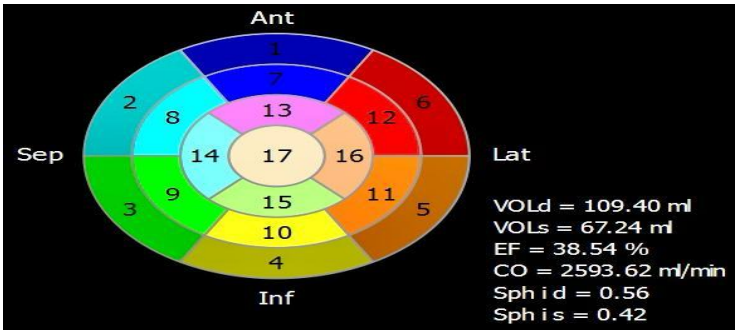

Figure 15: 4Dimensional Volumetric data derived from 4Dimensional XStrain Echocardiography. LVEF was 38.54 %.

Contrast Study

In the normal Apical 4CH view the LV endocardial borders were fuzzy and not clearly visible (Figure 16 A). Therefore, contrast study was carried out and it distinctly delineated the LV endocardial border (Figures 16 B, C). The contrast study exhibited marked thickness of LV apex and the lateral wall.

4 Chamber view (Diastole)

Normal Study		**Contrast Study**	
Apex	(D) 21.9 mm	Apex	(D) 19.0 mm
Apical lateral	(D) 15.4 mm	Apical lateral	(D) 18.0 mm
Mid lateral	(D) 19.6 mm	Mid lateral	(D) 18.1 mm
Basal lateral	(D) 17.0 mm	Basal lateral	(D) 17.6 mm
Apical septum	(D) 19.8 mm	Apical septum	(D) 11.3 mm
Mid septum	(D) 8.9 mm	Mid septum	11.5 mm
Basal septum	(D) 9.7 mm	Basal septum	12.4 mm
IVS/LVPW ratio = 2.19:1		IVS/LVPW ratio = 19:1	

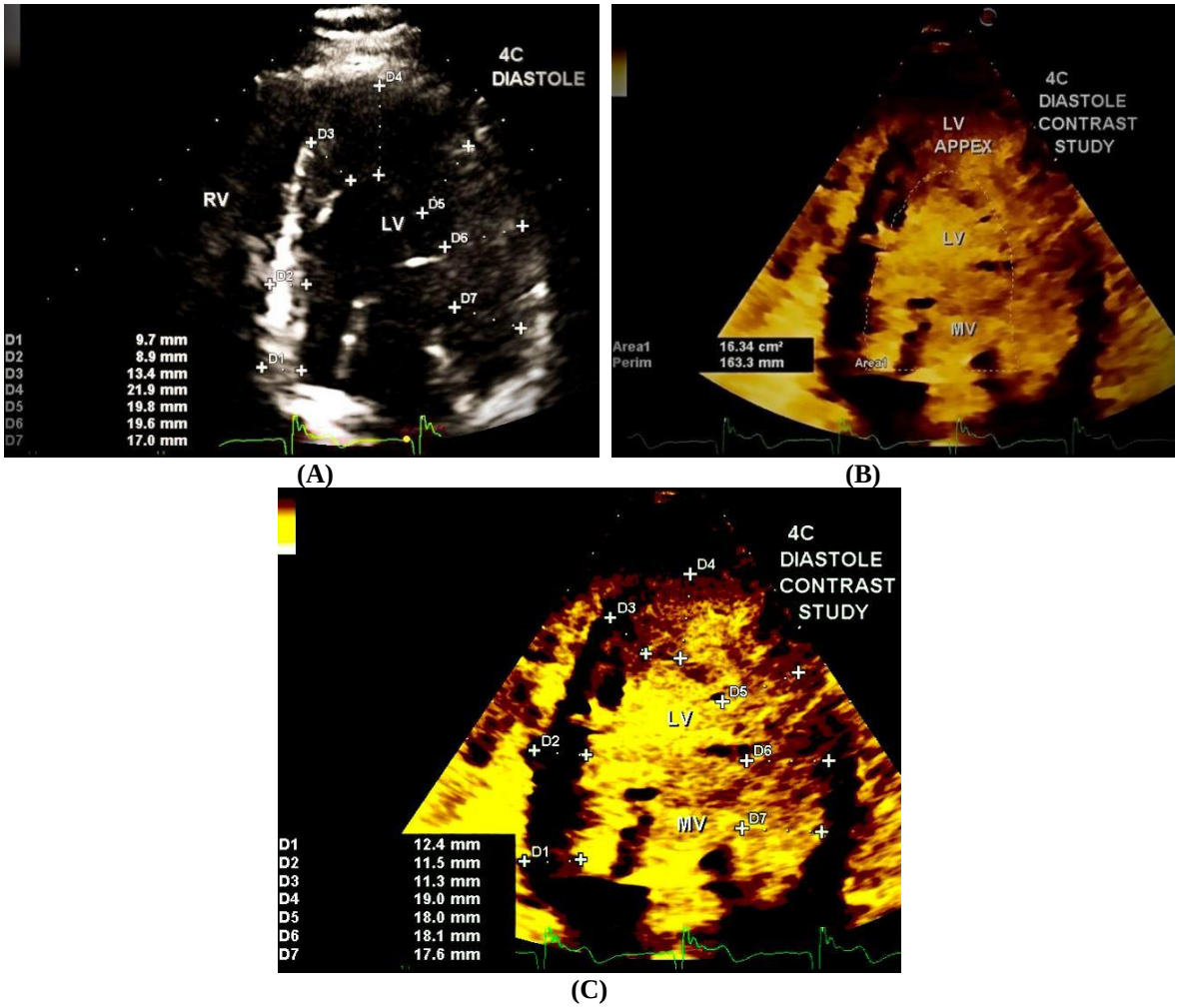

Figure 16: Contrast Study. (A) LV apical 4CH view depicting indistinct endocardial border; (B) Contrast study depicting the distinct LV endocardial border; (C) Contrast Study elucidating the measurements performed at different locations of LV myocardial thickness in diastole.

Table 3 exhibits LVEF variability with different methodologies of measurements. The 4Dimensional LVEF derived from 4DXStrain STE showed remarkable reduction of LVEF with a value of 38.54 % despite normal LVEF obtained from M-mode and Simpson's biplane method.

Table 3: LV ejection fraction variations by different methodologies

Technique	LVEF (%)
M-mode echocardiography	80%
Simpson's biplane method	51 %
4Dimensional LVEF derived from 4DXStrain echocardiography	38.54%
LVEF, left ventricular ejection fraction	

Speckle tracking echocardiography

Comprehensive speckle tracking echocardiography (STE) was accomplished by 4Dimensional XStrain technique. The values obtained of various LV strain parameters are enumerated (Table 4):

Table 4: 4Dimensional XStrain echocardiography - estimated values of LV strain parameters in our index patient.

LV strain Parameters	Strain (%)
Global longitudinal strain (GLS)	
AP 2C	-7.31
AP LAX (3CH)	-5.58
AP 4C	-7.97
Global strain	-6.96
AP, apical; 2C, two chamber; LAX, long axis; 4C, four chamber.	

There was severe reduction of global longitudinal strain (GLS) in apical 2CH, 3CH and 4CH view with a GLS value of -6.96 % (Figures 17, 18).

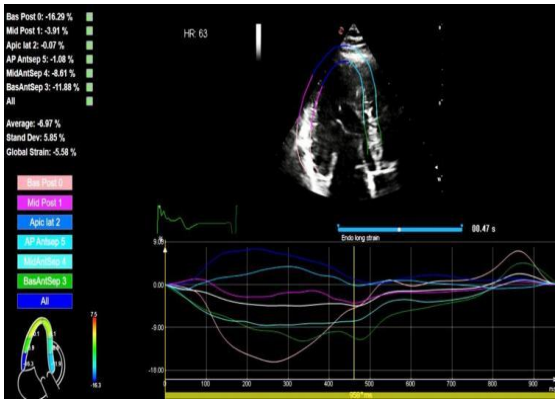

(A)

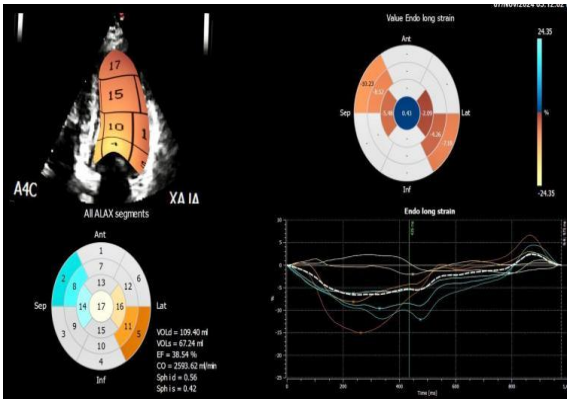

(B)

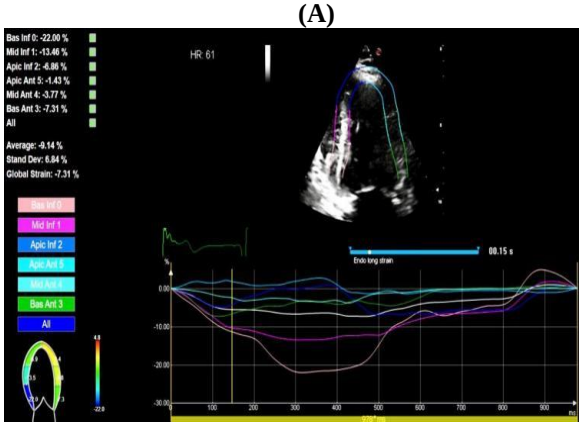

(C)

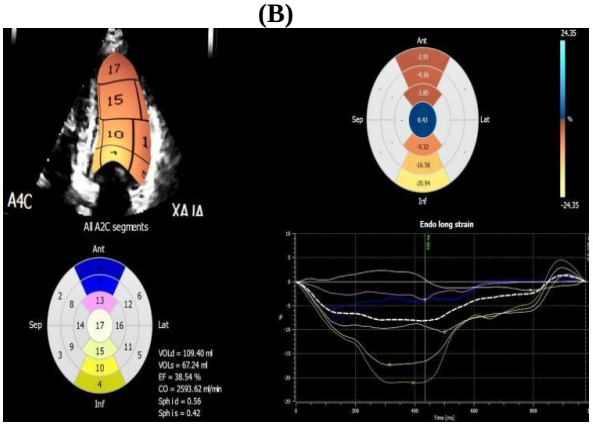

(D)

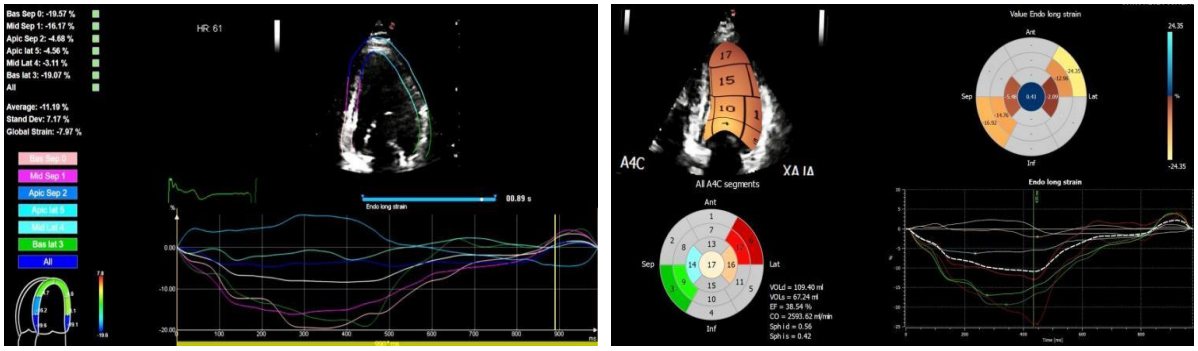

(E) **(F)**

Figure 17: Apical peak global longitudinal strain. (A) Apical LAX (3CH) GLS; (B) Apical LAX parametric maps (Bull's -eye displays) and graphs; (C) Apical 2CH GLS; (D) Apical 2CH parametric maps (Bull's -eye displays) and graphs; Apical 4CH GLS; (F) Apical 4CH parametric maps (Bull's -eye displays) and graphs.

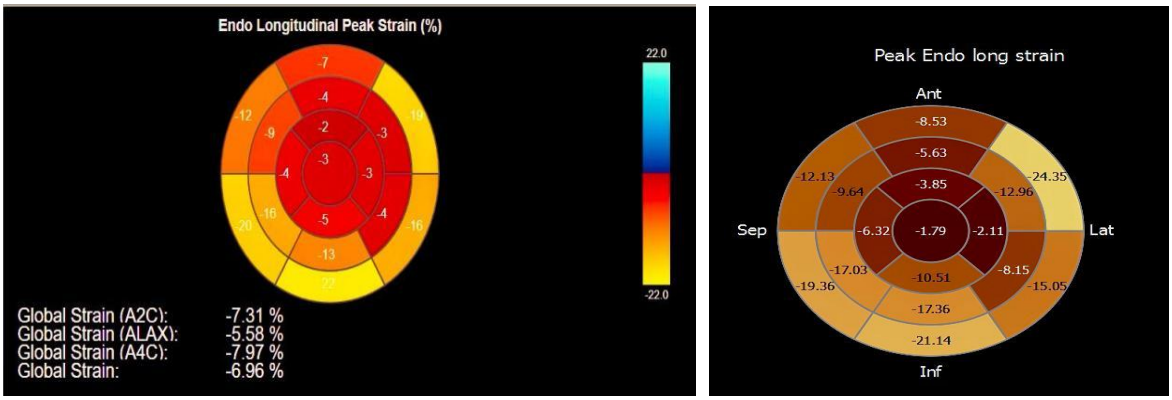

(A) **(B)**

Figure 18: Global Longitudinal Strain. (A) Bull's eye plot showing GLS values in apical 2C, LAX and 4C view; (B) Peak Segmental Strain values displayed in a 17 segment Bull's eye plot.

Table 5: 4Dimensional XStrain echocardiography estimation of LV segmental endocardial longitudinal strain

Bull's eye analysis		
Endo long strain (Peak)		
Bas Ant	-7.31	%
BasAntSep	-11.88	%
Bas Sep	-19.57	%
Bas Inf	-22.00	%
Bas Post	-16.92	%
Bas lat	-19.07	%
Mid Ant	-3.77	%
MidAntSep	-8.61	%
Mid Sep	-16.17	%
Mid Inf	-13.46	%
Mid Post	-3.91	%
Mid Lat	-3.11	%
Apic Ant	-1.89	%
Apic Sep	-4.32	%
Apic Inf	-5.36	%
Apic lat	-3.47	%
Apex	-3.11	%
Global Strain (A2C)	-7.31	%
Global Strain (ALAX)	-7.97	%
Global Strain (A4C)	-5.58	%
Global Strain	-6.96	%

Red squares depict significant reduction in strain values in multiple segments of LV

A 17 segment model of 4D XStrain global segmental strain, provided a detailed picture of regional myocardial function, by analyzing each segment individually, all with in a 4D (three-dimensional over time) imaging framework. The values obtained are mentioned in Table 5.

Summary of 2Dimensional transthoracic echocardiography

2D TTE in LX, SX Apical 4CH and Apical 3CH views demonstrated the presence of AHCM in our elderly asymptomatic patient. The thickness of LV apex was 21.9 mm and ratio of apex to posterior wall was 2.19:1. The LVEF determined by M-mode and Simpson's biplane method was normal, 80% and 51%, respectively. However, 4Dimensional volumetric analysis acquired from 4DXStrain STE validated a markedly reduced LVEF - 38.54 %.

Due to the presence of ill-defined LV endocardial borders, we conducted a contrast study to clearly demarcate the boundaries of LV. We found LV apical thickness of 19 mm and the ratio of apex to posterior wall was 1.9:1.

Additionally, speckle tracking imaging was executed by 4DXStrain STE technique which exhibited severe reduction of GLS and moreover, on segmental strain analysis, nearly all the segments illustrated substantial decline in strain values.

DISCUSSION

Hypertrophic cardiomyopathy (HCM) is mostly an autosomal dominant disease characterized predominantly by the detection of left ventricular (LV) hypertrophy in the absence of another cardiac, systemic, or metabolic disease [7].

Epidemiology

Hypertrophic cardiomyopathy is estimated to affect 1 out of 500 people. The AHCM has a different prevalence in cohorts of patients with HCM, which is relatively higher in Asian ethnicity. It is considered less common (8%) in Europe and North America with a majority (84%) of white race [8]. However, AHCM may occur more frequently in Asian race, in whom it is seen in up to 40% of HCM patients (21% in China [9], 30% in Japan [10], and 38% in Korea [11]) of patients with HCM.

AHCM is worldwide in distribution and affects males more frequently than females, with male-to-female ratios typically 1.6 to 2.8:1 [12]. Most commonly diagnosed in midlife [8], the early- and late-onset expressions are also known to occur.

Classification

According to the segments of LV hypertrophy, HCM can be classified into basal (also called classic HCM), midventricular, and apical. Apical hypertrophic cardiomyopathy (AHCM) is characteristic of hypertrophy predominantly involving the LV apex with giant negative T waves in the electrocardiogram and a "spade-like" configuration of the LV cavity on the LV ventriculogram [7, 13].

Morphologically AHCM can be subclassified into three subtypes [1]: pure, mixed, and relative AHCM (Figure 19).

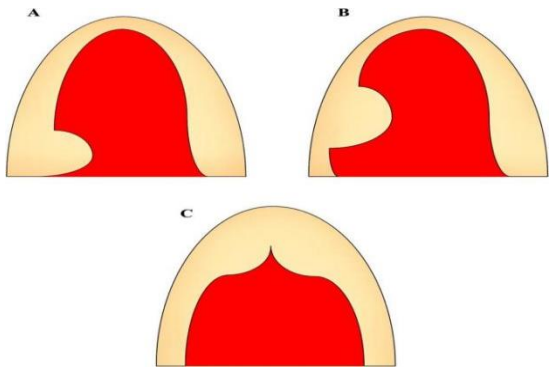

Figure 19: Diagrammatic illustration of AHCM variants. Variants of hypertrophic cardiomyopathy. Different morphologic types of hypertrophic cardiomyopathy: A basal, B midventricular, and C apical.

Pure AHCM presents with hypertrophy that is confined to the apex. Mixed AHCM displays both apical and septal hypertrophy but with the thickest apex. Finally, relative AHCM is believed to be an early AHCM phenotype. Individuals with relative AHCM do not meet conventional diagnostic criteria for AHCM but have similar imaging findings with the pure type. Relative AHCM can be diagnosed when electrocardiography shows characteristic precordial T-wave inversion and cardiac imaging techniques show apical wall thickness exceeding basal wall thickness, although failing to reach the cutoff of wall thickness ≥ 15 mm [14].

Clinical Diagnosis

Octo- and nonagenarians with AHCM are rare. Only few authors have reported AHCM in the elderly population [12, 15-17].

The differential diagnosis of AHCM should always be considered in elderly patients.

Table 6: Differential diagnosis of AHCM [18].

Disease	Imaging modalities
Coronary artery disease	Echocardiogram/coronary angiogram and LVG
Left ventricular apical tumors	Echocardiogram with contrast/CCT/CMRI
Left ventricular apical thrombus	Echocardiogram with contrast/CCT/CMRI
Isolated ventricular non-compaction	CMRI/CCT
Endomyocardial fibrosis	LVG/CMRI
AHCM: Apical hypertrophic cardiomyopathy; CMRI: Cardiac magnetic resonance imaging; LVG: Left ventriculography; CCT: Cardiac computed tomography.	

Diagnostic criteria

AHCM is described as an electrocardiographic pattern of giant negative T-waves (≥ 1 mV) together with a "spade-like configuration" of the LV cavity on the left ventriculography [20]. With advances in imaging techniques, the current definition mainly relies on demonstrating LV hypertrophy predominating in the LV apex, with the apical wall thickness ≥ 15 mm and a ratio of maximal apical to posterior wall thickness ≥ 1.5, based on echocardiography or CMR [5].

Standard TTE may miss this entity where a contrast echocardiography may be useful but cardiac MR imaging (CMR) is best [19, 20].

CMR is superior to TTE in detecting variants of HCM such as apical HCM, presence of focal hypertrophy, severe hypertrophy (>30 mm) and LV apical aneurysm. Patchy mid-wall-type delayed hyperenhancement of myocardium, on contrast-enhanced CMR, identifies fibrosis. It is associated with a higher risk of adverse LV remodelling and systolic dysfunction. Its association with ventricular tachycardia has been reported but its predictive value for sudden cardiac death is not clear [20, 21].

Electrocardiography

The trademark electrocardiographic finding for AHCM is LV hypertrophy with giant T waves, which are defined as T-waves ≥ 1 mV in any electrocardiography lead. These giant T waves are dynamic and will change over time, or even disappear, as a part of the natural history of AHCM [22]. The depth of T waves varies among patients, in a study of 208 AHCM patients, Yan et al [23] reported that 60 (28%) patients had giant T-waves, but only 11% of AHCM patients had giant T waves in a series from Mayo Clinic [12]. Although giant T-waves in the setting of LV hypertrophy are considered pathognomonic for AHCM, it is unlikely to rule out other causes of ST-T wave abnormalities, such as other types of HCM, coronary heart disease, medication effect (e.g., digoxin), and neurological diseases (e.g., subarachnoid hemorrhage).

Ambulatory 24- or 48-h electrocardiography is crucial to detect non-sustained ventricular tachycardia (NSVT), AF, and ventricular fibrillation. Eriksson et al [5] showed that Holter monitor recordings revealed NVST in 20 patients (23%) with AHCM, which was found to be correlated with the presence of fibrosis. Several studies have reported that the prevalence of AF was 11–17% [9, 10]. LA enlargement secondary to LV diastolic dysfunction in patients with AHCM can predict subsequent AF, which is prognostically adverse [24].

Transthoracic echocardiography

The preferred initial imaging test is Transthoracic Echocardiography and it is the most frequently utilized diagnostic modality [25].

Relative hypertrophy is defined as the absence of hypertrophy (wall thickness <14 mm) but with the apical wall thickness greater than the basal thickness (apex:base ratio (ABR) wall thickness >1). An apical-to-basal LV wall thickness ratio of 1.3 - 1.5 is diagnostic of apical HCM [26].

Apical HCM is characterized as concentric, circumferential hypertrophy of the entire apex due to apical left ventricular thickening of the anterior and posterior walls, resulting in a spade-like morphology of the left ventricular cavity during end diastole in LV long axis view of MRI and RAO projection of angiography [27].

The differential features of Japanese and non-Japanese type of AHCM is shown in the Table 7.

Table 7: Comparison of Japanese and Non-Japanese type of AHCM [28].

Japanese Type	Non-Japanese Type
Mostly seen in males	Elderly female in Asians and younger in West
"Pure" form is predominant	"Mixed" form is predominant
Asymptomatic and benign	Complications may occur
T-wave negativity is more pronounced	Less pronounced
Increased hypertrophy confined to apex	Segmental distribution may occur. Basal septal hypertrophy producing sub aortic obstruction in 50%, mid-septal hypertrophy with mid-cavity obstruction in 25%, apical septal hypertrophy with apical obliteration in 25% of cases. Occasionally, papillary muscle hypertrophy alone may be seen
Apical wall thickness lesser degree	More than Japanese in Americans

In transthoracic echocardiography, the lateral wall hypertrophy is more than the apical septum and producing a classical "ace of spades sign" in apical four chamber [29].

Kitaoka et al, demonstrated that the wall thickness at the apex was greater in Americans (23 ± 4 mm) than in the Japanese patients (18 ± 2 mm) [30].

In our patient, TTE in the apical 4CH and LX view showed thickness of LV apex and posterior wall to be 21.9 mm and 10 mm, respectively. The ratio of apical to posterior wall thickness was 2.19:1. The LVEF was 80 % and 51 % by M-mode and Simpson's biplane method, respectively, even though there was marked reduction of LVEF (38.54 %) by 4D volumetric analysis.

Contrast echocardiography

Because of frequent difficulties in visualizing the apical endocardium, 2D echocardiography may result in misdiagnosis, as it was reported that echocardiography failed to diagnose AHCM in 31.7% of patients [23]. Therefore, there is a need for an alternative imaging technique, and contrast echocardiography has been recommended as an alternative when 2D images are suboptimal [31]. The administration of echocardiographic contrast allows the excellent visualization of

LV morphology and the presence of an apical aneurysm.

In our index patient, on contrast study we identified thickness of LV apex to be 19 mm and the apical to posterior wall thickness ratio was 19:1. We did not find any LV apical wall motion abnormality or apical aneurysm.

Speckle tracking echocardiography

Regional LV function may be assessed non-invasively by measuring strain or systolic deformation. Recently, a method derived from the two-dimensional (2-D) echocardiogram, called "speckle tracking" of 2-D strain, has been developed to measure systolic strain [32]. Mutations of genes that code for contractile proteins of the sarcomere are responsible for the structural and functional changes seen in patients with HCM, and cause ventricular hypertrophy, myofibrillar disarray and interstitial fibrosis. In spite of the hyperdynamic systolic function seen by echo, 2-D strain detected a decrease in myocardial strain values [33].

In patients with HCM, Popović et al [34] have shown that 2-D strain was lower in patients whose MRI showed myocardial fibrosis than in patients without fibrosis.

The cherry-on-top strain pattern is classically seen in patients with cardiac amyloidosis due to amyloid deposition in the basal segments with relative apical sparing. In contrast, blueberry on top is observed in AHCM as the strain is spared in the LV base while the apex is distorted due to myocyte fiber disarray, increased loose connective tissue, and fibrosis, which are thought to interfere with force generation [35]. While the "inverse-amyloid" peak systolic strain pattern has been previously observed in patients with AHCM [36, 37], Alnaimat et al [38] in their study observed that time to peak strain seems to be a more robust tool in depicting the characteristic blueberry-on-top (BOT) phenotype in patients with AHCM and further opined that the BOT pattern can be manifested on both peak systolic and time to peak strain parametric maps. The authors also noted that time to peak strain showed a striking drop in value on ascending from base to apex as opposed to peak systolic strain values that had a modest drop. This drop or gradient of strain values reflects on the bull's-eye plot color mapping as a shift from true red to pink (for modest gradients) or from true red to blue (for steeper gradients). The final appearance of the strain bull's eye plot therefore may vary from patient to patient and among different echocardiographic vendors [38]. The recognition of such variability is important for accurate interpretation of the BOT phenomenon in clinical practice. It is important to recognize that the BOT strain pattern is not specific for AHCM since patients with ischemic heart disease and apical aneurysm/dyskinesia can have a similar strain pattern. Therefore, the BOT strain pattern could be utilized as a suggestive feature of AHCM in the presence of appropriate diagnostic background [38].

In the HUNT study of 1266 healthy subjects [39], the authors acknowledged that the normal range of GLS was from -16 % to -22%. It is noteworthy that in healthy subjects, the strain values tend to increase as we ascend from base to apex [32, 39]. In paradoxical strain pattern there is reversal of this phenomenon and the strain values show attenuation as we move upwards from base to apex [40, 41]. This finding correlates with pathologic ventricular hypertrophy extending beyond the apex into the mid-ventricular segments and appears to support the diagnosis of AHCM.

In our case, we did not observe any BOT phenomenon in the Bull's eye plot of peak systolic strain or time to peak systolic strain values (Figure 20), although there was severe drop in peak systolic strain values and paradoxical strain arrangement was distinctly elucidated as demonstrated by Reddy et al [41]. Moreover, there was striking delay in time to peak strain values on ascending from base to apex along with severe reduction of GLS predominantly affecting the apical & mid basal segments.

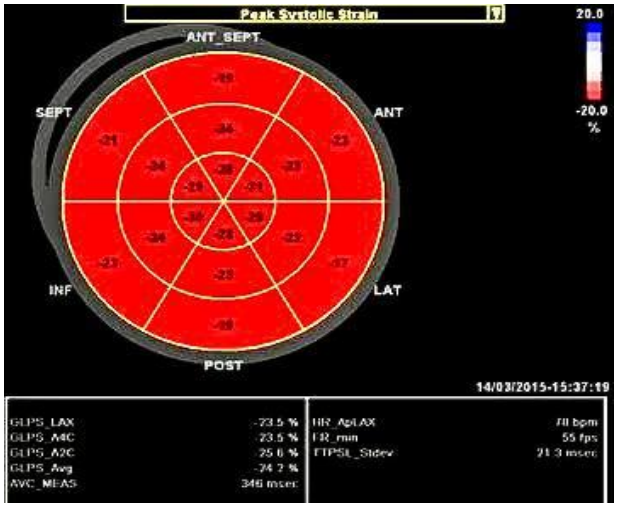

(A)

Bull's eye plot in a healthy subjected [39]

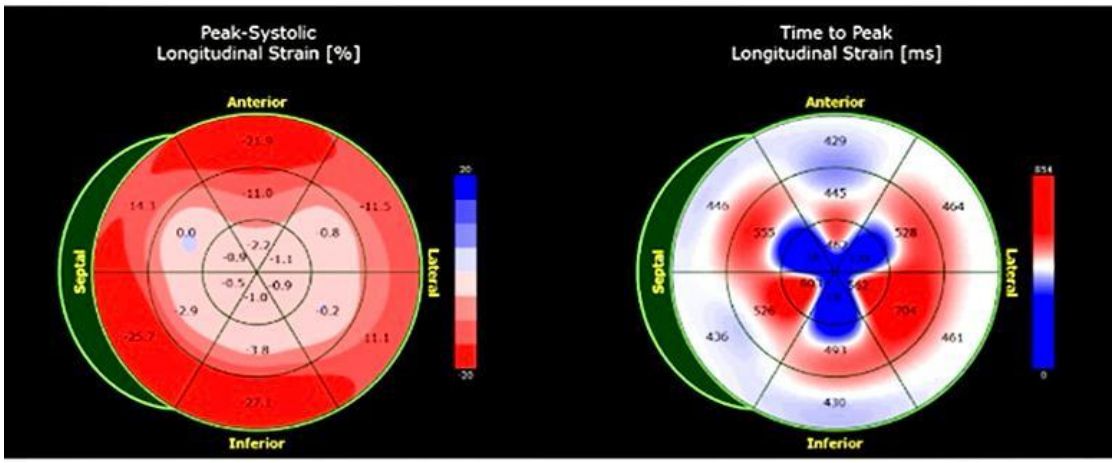

(B) **(C)**

Bull's eye plot in a patient of AHCM [38]

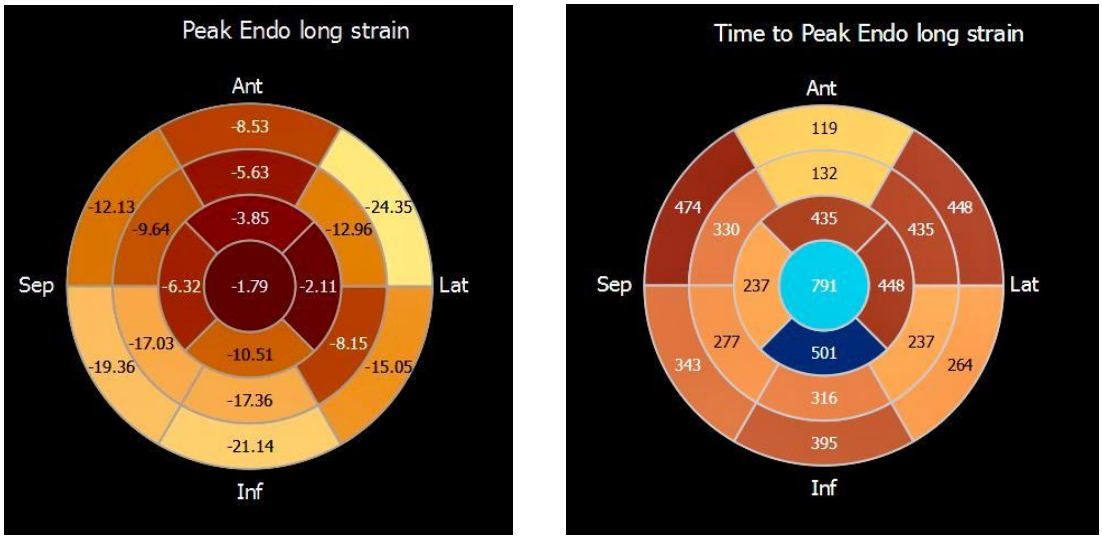

(D) **(E)**

Bull's eye plot in our patient

Figure 20: Bull's eye plot on speckle tracking echocardiography: (A) in a healthy subject; (B) peak systolic strain and (C) time to peak systolic strain in a patient of AHCM; (D) peak systolic longitudinal strain and (E) time to peak systolic strain in our case.

Late Onset AHCM

The reason for the late and gradual onset of AHCM compared to HCM variants is not established [42]. Compared to non-apical HCM, AHCM seems to carry a more favourable prognosis [43].

CONCLUSION

The diagnosis of AHCM can be challenging, necessitating additional expensive imaging modalities such as cardiac MRI, contrast-enhanced echocardiography, or left ventricular angiography. Two-dimensional strain, on the other hand, can be rapidly computed from conventional echocardiographic images and appears to be a promising novel application, particularly suited for the diagnosis of suspected AHCM. While clearly in need of further clinical validation, it could complement the role of contrast echocardiography and mitigate the need for more expensive or invasive imaging alternatives in patients with otherwise non-diagnostic or equivocal echo exams.

Declaration by Authors

Acknowledgement: None
Source of Funding: None
Conflict of Interest: The authors declare no conflict of interest.

REFERENCES

1. Hughes RK, Knott KD, Malcolmson J, Augusto JB, Mohiddin SA, Kellman P, et al. Apical hypertrophic cardiomyopathy: the variant less known. J Am Heart Assoc, 2020;9: e015294.
2. Paluszkiewicz J, Krasinska B, Milting H, Gummert J, Pyda M. Apical hypertrophic cardiomyopathy: diagnosis, medical and surgical treatment. Kardiochir Torakochirurgia Pol 2018; 15:246-53.
3. Sakamoto T, Tei C, Murayama M, Ichiyasu H, Hada Y. Giant T wave inversion as a manifestation of asymmetrical apical hypertrophy (AAH) of the left ventricle. Echocardiographic and ultrasono-cardiotomographic study. Jpn Heart J, 1976;17:611-6293.
4. Jan MF, Todaro MC, Oreto L, Jamil Tajik A. Apical hypertrophic cardiomyopathy: present status. Int J Cardiol, 2016;222:45-759.
5. Eriksson MJ, Sonnenberg B, Woo A, Rakowski P, Parker TG, Douglas Wigle E, et al. Long-term outcome in patients with apical hypertrophic cardiomyopathy. J Am Coll Cardiol, 2002;39:638-645.
6. Sakamoto T, Amano K, Hada Y, Tei C, Takenaka K, Hasegawa I, et al. Asymmetric apical hypertrophy: ten years' experience Postgrad Med J, 1986;62:567-570.
7. Ommen SR, Mital S, Burke MA, Day SM, Deswal A, Elliott P, et al. 2020 AHA/ACC guideline for the diagnosis and treatment of patients with hypertrophic cardiomyopathy: a report of the American College of Cardiology/American Heart Association Joint Committee on clinical practice guidelines. J Am Coll Cardiol. 2020;76: e159–e240.
8. Neubauer S, Kolm P, Ho CY, Kwong RY, Desai MY, Dolman SF, et al. Distinct subgroups in hypertrophic cardiomyopathy in the NHLBI HCM Registry. J Am Coll Cardiol. 2019; 74:2333–2345.
9. Yin Y, Hu W, Zhang L, Wu D, Yang C, Ye X. Clinical, echocardiographic and cardiac MRI predictors of outcomes in patients with apical hypertrophic cardiomyopathy. Int J Cardiovasc Imaging. 2022; 38:643–651.
10. Kubo T, Kitaoka H, Okawa M, Hirota T, Hoshikawa E, Hayato K, et al. Clinical profiles of hypertrophic cardiomyopathy with apical phenotype–comparison of pure-apical form and distal-dominant form. Circ J. 2009; 73:2330–2336.
11. Moon J, Shim CY, Ha JW, Cho IJ, Kang MK, Yang WI, et al. Clinical and echocardiographic predictors of outcomes in patients with apical hypertrophic cardiomyopathy. Am J Cardiol. 2011; 108:1614–1619.
12. Klarich KW, Attenhofer Jost CH, Binder J, Connolly HM, Scott CG, Freeman WK, et al. Risk of death in long-term follow-up of patients with apical hypertrophic cardiomyopathy. Am J Cardiol. 2013; 111:1784–1791.
13. Elliott PM, Anastasakis A, Borger MA, Borggrefe M, Cecchi F, et al. ESC guidelines on diagnosis and management of hypertrophic cardiomyopathy: the task force for the diagnosis and management of hypertrophic cardiomyopathy of the

European Society of Cardiology (ESC) Eur Heart J. 2014;35:2733–2779.
14. Flett AS, Maestrini V, Milliken D, Fontana M, Treibel TA, Harb R, et al. Diagnosis of apical hypertrophic cardiomyopathy: T-wave inversion and relative but not absolute apical left ventricular hypertrophy. Int J Cardiol. 2015; 183:143–148.
15. Stöllberger C, Yoshida T, Finsterer J. Never too old for a change. ECG in a nonagenarian with apical hypertrophic cardiomyopathy, aneurysm, and encephalomyopathy. Herz. 2015; 40:96–100.
16. Maron BJ, Desai MY, Nishimura RA, Spirito P, Rakowski H, Towbin JA, et al. Diagnosis and evaluation of hypertrophic cardiomyopathy: JACC State-of-the-Art Review. J Am Coll Cardiol. 2022; 79:372–389.
17. Støylen A, Sletvold O, Skjaerpe T. Post systolic shortening in nonobstructive hypertrophic cardiomyopathy with delayed emptying of the apex: a Doppler flow, tissue Doppler and strain rate imaging case study. Echocardiography. 2003; 20:167–171.
18. Yusuf SW, Bathina JD, Banchs J, Mouhayar EN, Daher IN. Apical hypertrophic cardiomyopathy. World J Cardiol 2011; 3:256-259.
19. Yamaguchi H, Ishimura T, Nishiyama S, Nagasaki F, Nakanishi S, Takatsu F, et al. Hypetrophic nonobstructive cardiomyopathy with giant negative T waves (apical hypertrophy): ventriculographic and echocardiographic features in 30 patients. Am J Cardiol. 1979; 44:401-412.
20. Hansen MW, Merchant N. MRI of hypertrophic cardiomyopathy: part I, MRI appearances. AJR 2007; 189:1335–43.
21. Maron MS. Clinical utility of cardiovascular magnetic resonance imaging in hypertrophic cardiomyopathy. J Cardiovasc Magn Reson 2012; 14:13.
22. Koga Y, Katoh A, Matsuyama K, Ikeda H, Hiyamuta K, Toshima H, et al. Disappearance of giant negative T waves in patients with the Japanese form of apical hypertrophy. J Am Coll Cardiol. 1995; 26:1672–1678.
23. Yan L, Wang Z, Xu Z, Li Y, Tao Y, Fan C. Two hundred eight patients with apical hypertrophic cardiomyopathy in China: clinical feature, prognosis, and comparison of pure and mixed forms. Clin Cardiol. 2012; 35:101–106.
24. Chen X, Dong JZ, Du X, Wu JH, Yu RH, Long DY, et al. Long-term outcome of catheter ablation for atrial fibrillation in patients with apical hypertrophic cardiomyopathy. J Cardiovasc Electrophysiol. 2018; 29:951–957.
25. Stainback RF. Apical Hypertrophic Cardiomyopathy. Texas Heart Institute Journal, 2012;39:747-749.
26. Chun EJ, et al. Hypertrophic Cardiomyopathy. Assessment with MR imaging and Multi-Detector CT. Radiographics, 2010;30:1309-1328.
27. Suzuki J, Watanabe F, Takenaka K, et al. New Subtype of Apical Hypertrophic Cardiomyopathy Identified with Nuclear Magnetic Resonance Imaging as an Underlyiong Cause of Markedly Inverted T Waves. Journal of American College of Cardiology, 1993;22:1175-1181.
28. Muthiah, R. Apical Left Ventricular Hypertrophic Cardiomyopathy: A Case Report. Case Reports in Clinical Medicine, 2016;5:308-329.
29. Chaturvedi H. Apical Hypertrophic Cardiomyopathy with Hemodynamically Unstable Ventricular Arrhythmia: Atypical Presentation. EC (E-CRONICON) Cardiology, 2015;2:106-110.
30. Kitaoka H, Doi Y, Casey SA, Hitomi N, Furuno T, & Maron BJ. Comparison of prevalence of apical hypertrophic cardiomyopathy in Japan and the United States. The American journal of cardiology, 2023;92:1183-1186.
31. Senior R, Becher H, Monaghan M, Agati L, Zamorano J, Vanoverschelde JL, et al. Clinical practice of contrast echocardiography: recommendation by the European Association of Cardiovascular Imaging (EACVI). Eur Heart J Cardiovasc Imaging. 2017; 18:1205–1205.
32. Leitman M, Lysyansky P, Sidenko S, Shir V, Peleg E, Binenbaum M, Kaluski E, Krakover R, Vered Z. Two-dimensional strain-a novel software for real-time quantitative echocardiographic assessment of myocardial function. J Am Soc Echocardiogr 2004; 17:1021-1029.
33. Saccheri MC, Cianciulli TF, Morita LA, Méndez RJ, Beck MA, Guerra JE, Cozzarin A, Puente LJ, Balletti LR, Lax JA. Speckle tracking echocardiography to assess

regional ventricular function in patients with apical hypertrophic cardiomyopathy hypertrophic cardiomyopathy.World J Cardiol. 2017; 9:363-370.
34. Popović ZB, Kwon DH, Mishra M, Buakhamsri A, Greenberg NL, Thamilarasan M, Flamm SD, Thomas JD, Lever HM, Desai MY. Association between regional ventricular function and myocardial fibrosis in hypertrophic cardiomyopathy assessed by speckle tracking echocardiography and delayed hyperenhancement magnetic resonance imaging. J Am Soc Echocardiogr 2008; 21:1299-1305.
35. Carasso S, Rakowski H. Chapter 23-hypertrophic cardiomyopathy. Diastology 2008;287-99.
36. Liu D, Hu K, Nordbeck P, Ertl G, Störk S, Weidemann F. Longitudinal strain bull's eye plot patterns in patients with cardiomyopathy and concentric left ventricular hypertrophy. Eur J Med Res 2016; 21:21.
37. Mihos CG, Horvath SA, Fernandez R, Escolar E. Left ventricular strain and myocardial work in apical hypertrophic cardiomyopathy. J Thorac Dis 2023; 15:3197-207.
38. Alnaimat S, Mascara M, Lygouris G, & Biederman RWW. Blueberry-on- Top Phenomenon in Apical Variant Hypertrophic Cardiomyopathy. CASE (Philadelphia, Pa.), 2024;8:296-302.
39. Dalen H, Thorstensen A, Aase SA, Ingul CB, Torp H, Vatten LJ, Stoylen A. Segmental and global longitudinal strain and strain rate based on echocardiography of 1266 healthy individuals: the HUNT study in Norway. Eur J Echocardiogr. 2010; 11:176-83.
40. Serri K, Reant P, Lafitte M, Berhouet M, Le Bouffos V, Roudaut R et al. Global and regional myocardial function quantification by two-dimensional strain: application in hypertrophic cardiomyopathy. J Am Coll Cardiol. 2006; 47:1175-81.
41. Reddy M, Thatai D, Bernal J, Pradhan J, Afonso L. Apical hypertrophic cardiomyopathy: potential utility of Strain imaging, European Journal of Echocardiography. 2008; 9:560-562.
42. Towe EC, Bos JM, Ommen SR, Gersh BJ, Ackerman MJ. Genotype-phenotype correlations in apical variant hypertrophic cardiomyopathy. Congenit Heart Dis 2015;10: E139–45.
43. Itzhaki Ben Zadok O, Hasdai D, Witberg G, Shapira Y, Vaturi M, Monakier D. Calculated risk for sudden cardiac death in patients with apical versus nonobstructive nonapical hypertrophic cardiomyopathy. Am J Cardiol 2018; 122:1551–1556.

How to cite this article: Akhil Mehrotra, Faiz Illahi Siddiqui. Yamaguchi syndrome (ace of spades) in an elderly male. case report and literature review. *International Journal of Science & Healthcare Research.* 2024; 9(4): 435-453. DOI: *10.52403/ijshr.20240449*

******